interaction gives about 400 MeV for the optical-potential well depth, or about 8 times the empirical value. However, it might be noted that only the monopole part of the interaction contributes, and we have already seen that this predicts an excitation cross section for the 0^+ level at 1.75 MeV which is an order of magnitude larger than that observed. It remains to be seen whether these gross discrepancies are due to the inadequacy of the model potential for the monopole part of the interaction, to the neglect of exchange effects, or to some other cause.

Some of these questions may be answered by a similar analysis of proton scattering data from other nuclei whose wave functions are probably well described by the shell model, such as those of the $1f_{7/2}$ shell.[31]

ACKNOWLEDGMENTS

We wish to express our appreciation to Margaret Stautberg, D. Zurstadt, and D. Petersen for assistance in data taking and data analysis, and to the staffs of the University of Colorado Nuclear Physics Laboratory and the University of Colorado Computing Center. We are indebted to R. M. Drisko for making available the optical-model code HUNTER and the distorted-wave code JULIE.

[31] W. S. Gray, R. A. Kenefick, and J. J. Kraushaar, Nucl. Phys. **67**, 542 (1965); *ibid.* **67**, 565 (1965).

PHYSICAL REVIEW VOLUME 142, NUMBER 3 FEBRUARY 1966

Shell-Model Form Factors for the $^{90}Zr(p,p')$ Reaction*

M. B. JOHNSON,† L. W. OWEN,‡ AND G. R. SATCHLER
Oak Ridge National Laboratory, Oak Ridge, Tennessee
(Received 29 September 1965)

The application of the shell model to the $^{90}Zr(p,p')$ reaction is described. The nuclear matrix elements, and particularly the radial form factors, are discussed. Interactions of Gaussian and Yukawa form between projectile and target nucleons are used. They are assumed to be central, but spin and isospin dependence is included. The shell-model orbitals are calculated for a potential of the Woods-Saxon shape. The effects of parameter variations and of corrections such as may be due to nonlocality of the potentials are studied in some detail. It is shown how the data for the $^{90}Zr(p,p')$ reaction favor a Yukawa interaction with a range of about 1 F.

I. INTRODUCTION

THE preceding paper[1] described the results of measurements on the $^{90}Zr(p,p')$ reaction at 18.8 MeV, and compared them with theoretical predictions based on the nuclear-shell model. In the present paper we examine in more detail some aspects of this model, in particular the radial form factors which arise from the nuclear matrix elements. Various features, such as the effects of including nonlocality corrections, are explored so that a better assessment can be made of the fits to experimental data and the significance of the parameters so obtained.

In order to apply the shell model, we need to assume an interaction v_{ip} between the projectile p and each target nucleon i. At high energies (say, 100 MeV or greater) it is reasonable to invoke the impulse approximation,[2] in which v_{ip} is replaced by the scattering amplitude t_{ip} for two free nucleons. However, at the lower energies with which we are concerned here, the corrections to this simple prescription are likely to be so large it is more profitable, at least initially, to regard v_{ip} as an effective interaction for which we may try various phenomenological models. The parameters of the model interaction are then to be determined by fitting to experimental data. Before this can be done we must have some knowledge of the wave functions for the target nucleus which is to be excited.

^{90}Zr is quite appropriate for this purpose since it possesses a set of excited states which appear to be due to relatively pure $(g_{9/2})^2$ and $(g_{9/2}p_{1/2})$ configurations for the last two protons.[3] The first of these configurations has states of spin 0^+, 2^+, 4^+, 6^+, and 8^+ whose excitation selects out the corresponding multipoles of the effective interaction and provides a detailed probe of its structure.

The information contained in the experimental data is of two kinds. On the one hand we have the cross-section magnitudes, and in particular the relative mag-

* Research sponsored by the U. S. Atomic Energy Commission under contract with Union Carbide Corporation.

† Participant in Student Cooperative Program from Virginia Polytechnic Institute, Blacksburg, Virginia.

‡ Permanent address: Physics Department, University of Tennessee, Knoxville, Tennessee.

[1] W. S. Gray, R. A. Kenefick, J. J. Kraushaar, and G. R. Satchler, preceding paper, Phys. Rev. **142**, 735 (1966).

[2] A. K. Kerman, H. McManus, and R. M. Thaler, Ann. Phys. (N. Y.) **8**, 551 (1959); R. M. Haybron and H. McManus, Phys. Rev. **136**, B1730 (1964).

[3] B. F. Bayman, A. S. Reiner, and R. K. Sheline, Phys. Rev. **115**, 1627 (1959); I. Talmi and I. Unna, Nucl. Phys. **19**, 225 (1960).

nitudes for sets of states such as the one just mentioned. These provide information about the multipole decomposition of the interaction (and hence, for example, its range and possibly its shape) as well as its over-all strength. On the other hand we have the angular distributions for each transition. The qualitative shapes of these are known to be determined largely by the multipolarity (angular-momentum transfer) and by the elastic distortions (described by the optical-model potential). Poor quality or incomplete data will then tell us little else. However, measurements with the kind of accuracy which is readily obtainable today could often distinguish between the predictions of various forms of the model—for example, different configuration assignments.

The effective interaction which should appear in our calculations is probably very complicated and akin to the reaction matrix effective interaction which appears in the work of Brueckner[4] and others.[2,5] We could reasonably expect it to be nonlocal, and dependent upon the relative angular momentum of the interacting pair. Further, it may well depend upon the positions of the two nucleons within the nucleus as well as their relative separation; the effective interaction is different when both are deeply imbedded in the nucleus from what it is when both are outside the bulk of the nucleus.[4,5] These differences may also depend upon the orbit occupied by the target nucleon.[4] We mention these things so as to emphasize the possible deficiencies of the simple local interaction we use which depends only upon the separation of the two interacting nucleons. We also neglect the spin-orbit and tensor interactions which are known to be present in the interaction between free nucleons. Simplicity is the main justification for this procedure, which is closely analogous to that followed in shell-model calculations of bound states. A more general interaction would contain more parameters than could be determined reasonably at this time.

We also assume that we can neglect exchange contributions to the inelastic scattering in which the projectile is captured and a target nucleon is ejected (except insofar as the effects of these are included in the effective interaction used). These exchange terms involve more complicated overlap integrals for the nuclear wave functions, and there is some justification for their neglect from calculations on the $^{28}Si(n,p)$ reaction.[6]

II. THE INTERACTION

The distorted-wave amplitude[1,7] for inelastic scattering[8] from an initial state $|i\rangle$ to a final state $|f\rangle$ includes as a factor the nuclear matrix element $\langle f|V|i\rangle$. The same factor appears in the coupling terms when the coupled-equations technique[9] is used. In the present model $V=\sum_i v_{ip}$, where i refers to a target nucleon. For the nucleon-nucleon interaction we take the central potential

$$v_{ip}=-(V_0+V_1\boldsymbol{\sigma}_i\cdot\boldsymbol{\sigma}_p)g(r_{ip}), \tag{1}$$

where

$$V_S=V_{S\alpha}+V_{S\beta}\boldsymbol{\tau}_i\cdot\boldsymbol{\tau}_p, \tag{2}$$

and r_{ip} is the distance between the two nucleons, $r_{ip}=|\mathbf{r}_i-\mathbf{r}_p|$. We make the usual multipole expansion[10] of $g(r_{ip})$ in the coordinates $\mathbf{r}_i$ and $\mathbf{r}_p$,

$$g(r_{ip})=4\pi\sum_{LM}g_L(r_i,r_p)Y_L{}^M(\theta_i\phi_i)Y_L{}^M(\theta_p\phi_p)^*. \tag{3}$$

Each term in this expansion can give rise to the transfer of (orbital) angular momentum L to the nucleus, and corresponds to a parity change of $(-)^L$. In addition, the second term of the potential (1) can give an additional transfer of $S=1$ unit through what we shall call spin flip. The total angular-momentum transfer J is then the vector sum of these,

$$\mathbf{J}=\mathbf{L}+\mathbf{S},$$

where $S=0$ (so $J=L$) for the first term of the interaction (1), and $S=1$ (so $J=L$, $L\pm1$) for the second term. This multipole expansion may be expressed by using the tensors[10]

$$T_{LSJ,\mu}(\theta\phi,\boldsymbol{\sigma})=\sum_M i^L Y_L{}^M(\theta\phi)S_{S,\mu-M}(\boldsymbol{\sigma})\langle LSM,\mu-M|J\mu\rangle \tag{4}$$

if we choose $S_{00}=1$ and $S_{1\lambda}=\sigma_\lambda$. Then, of course, $T_{L0L,M}=i^L Y_L{}^M$. With Eq. (3) the interaction (1) may then be written

$$v_{ip}=-4\pi\sum_{LSJ}(-)^{J+S-\mu}V_S g_L(r_i,r_p)\times T_{LSJ,\mu}(\theta_i\phi_i\boldsymbol{\sigma}_i)T_{LSJ,-\mu}(\theta_p\phi_p\boldsymbol{\sigma}_p). \tag{5}$$

It follows that the nuclear matrix element $\langle f|V|i\rangle$ may be expressed[7,8] in terms of the reduced matrix elements[10] of the tensors (4),

$$\langle I_f\|\textstyle\sum_i g_L(r_i,r_p)T_{LSJ}(\theta_i\phi_i\boldsymbol{\sigma}_i)\|I_i\rangle, \tag{6}$$

where I_i, I_f are the spins of the initial and final states. Of course, we have the selection rule

$$|I_i-I_f|\leq J\leq I_i+I_f.$$

[4] See, for example, K. A. Brueckner, A. M. Lockett, and M. Rotenberg, Phys. Rev. **121**, 255 (1961).
[5] N. C. Francis, D. T. Goldman, and C. R. Lubitz, Ann. Phys. (N. Y.) **29**, 232 (1964); I. M. Green and S. A. Moszkowski, Phys. Rev. **139**, B790 (1965).
[6] A. Agodi and G. Schiffrer, Nucl. Phys. **50**, 337 (1964).
[7] See, for example, G. R. Satchler, Nucl. Phys. **55**, 1 (1964); we use the notation of this reference.
[8] R. H. Bassel, G. R. Satchler, R. M. Drisko, and E. Rost, Phys. Rev. **128**, 2693 (1962).
[9] B. Buck, Phys. Rev. **130**, 712 (1963).
[10] D. M. Brink and G. R. Satchler, *Angular Momentum* (Oxford University Press, New York, 1962). We use the Wigner-Eckart theorem in the form

$$\langle I'M'|T_{j\mu}|IM\rangle=\langle IjM\mu|I'M'\rangle\langle I'||T_j||I\rangle.$$

Given specific nuclear wave functions these matrix elements may be evaluated by standard techniques.[10,11] They remain functions of the radial coordinate r_p. Since the operator appearing in the element (6) is a single-particle operator, it only connects configurations which differ in the state of at most one nucleon. If only one configuration in both initial and final states contributes to the transition, the element (6) factors into a radial part and a spin-angle part.

$$\langle I_f\|\textstyle\sum_i g_L T_{LSJ}\|I_i\rangle=(M_L\delta_{S0}+N_{LJ}\delta_{S1})I_L(r_p), \quad (7)$$

where the multipole coefficients[12]

$$M_L=\langle I_f\|\textstyle\sum_i i^L Y_L(\theta_i\phi_i)\|I_i\rangle, \quad (8a)$$

and

$$N_{LJ}=\langle I_f\|\textstyle\sum_i T_{L1J}(\theta_i\phi_i\sigma_i)\|I_i\rangle, \quad (8b)$$

are properties of the nuclear wave functions only, and are indepednent of the assumed interaction. The choice of interaction affects only the radial form factor, which is just

$$I_L(r_p)=\int u_2(r_i)u_1(r_i)g_L(r_i,r_p)r_i^2dr_i. \quad (9)$$

The $u_k(r)$ are the radial parts of the single-particle wave functions involved in the transition; the subscript k stands for the set of quantum numbers n_k, l_k, j_k. The I_L depends upon these quantum numbers, but we omit the labels for simplicity.

If the nuclear wave functions involve mixed configurations, with more than one contributing, the element (6) is simply a sum of terms (7) weighted by the corresponding mixing coefficients. Most of the present paper is concerned with transitions which can be expressed as in Eq. (7). Further, for an even target like ^{90}Zr with zero spin and even parity, $I_i=0$, and the value of J is restricted to $J=I_f$. "Normal" parity states, with spin J and parity $(-)^J$ can then only be excited with a transfer of $L=J$. States with non-normal parity, $(-)^{J+1}$, must be excited with $L=J\pm1$; this requires spin flip. A spin-independent ($S=0$) interaction will not excite these non-normal parity states.

So far we have neglected to discuss the consequences of the isospin dependence of the interaction. The second term of the interaction (2) also results in matrix elements of the form (6) except that each term of the operator is multiplied by τ_i. However, in the present work we do not need such isovector operators; the isoscalar form (6) is sufficient provided we take the appropriate expectation value of the operator (2). If only protons are excited in the target this becomes $V_S=V_{S\alpha}\pm V_{S\beta}$, with the upper sign for a proton projectile, the lower sign for a neutron projectile. Similarly, states obtained by only exciting target neutrons have $V_S=V_{S\alpha}\mp V_{S\beta}$. It would be interesting in such cases to compare the results of neutron and proton scattering; in principle, one could then determine $V_{S\alpha}$ and $V_{S\beta}$ separately. The only other case dealt with here concerns hole-particle excitations of the doubly-closed-shell configuration in which the $g_{9/2}$ shell is filled for neutrons, empty for protons. Neutrons and protons participate equally in hole-particle excitations which do not involve the $g_{9/2}$ orbit, in "$T=0$" and "$T=1$" combinations; the $T=0$ states are expected to be lower in energy. Only the isoscalar interaction contributes to exciting $T=0$, so $V_S=V_{S\alpha}$, and only the isovector, with $V_S=V_{S\beta}$, contributes to the $T=1$ transitions.

III. THE NUCLEAR MATRIX ELEMENTS

However complicated the nuclear wave functions, the nuclear matrix element (6) can be expressed in terms of the multipole coefficients or matrix elements (8) taken between the various configurations involved. The evaluation of such elements has been discussed in detail elsewhere[10,11] and we shall merely quote the results for the cases of interest here. As already remarked, the operators only connect configurations which differ in the state of at most one nucleon, hence the results will contain as a factor the single-particle matrix element for the transition from the orbit (l_1j_1) to the orbit (l_2j_2) [only the radial factor (9) depends on the principal quantum numbers n_k],

$$\langle l_2j_2|\,|T_{LSJ}|\,|l_1j_1\rangle=i^{l_2-l_1+L}(-)^{j_1-1/2}\times\left[\frac{(2j_1+1)(2L+1)}{4\pi}\right]^{1/2}a_{LSJ}\begin{pmatrix} j_2 & j_1 & J\\ \frac{1}{2} & -\frac{1}{2} & 0\end{pmatrix}, \quad (10)$$

where $a_{L0L}=1$, and for $S=1$

$$\begin{aligned} a_{L1L}&=[(l_1-j_1)(2j_1+1)-(l_2-j_2)(2j_2+1)]/[L(L+1)]^{1/2},\\ a_{L1L-1}&=-[L+(l_1-j_1)(2j_1+1)+(l_2-j_2)(2j_2+1)]/[L(2L+1)]^{1/2}, \quad (11)\\ a_{L1L+1}&=[L+1-(l_1-j_1)(2j_1+1)\\ &\quad-(l_2-j_2)(2j_2+1)]/[(L+1)(2L+1)]^{1/2}. \end{aligned}$$

The following selection rules apply to these matrix elements,

$$|l_1-l_2|\leq L\leq l_1+l_2, \quad |j_1-j_2|\leq J\leq j_1+j_2.$$

Parity conservation demands that $L+l_1+l_2$ be even. The single-particle wave functions are defined as

$$|lj,m\rangle=\textstyle\sum_\lambda u_{nlj}(r)i^lY_l^{m-\lambda}(\theta\phi)\chi_{\frac{1}{2}\lambda}(\sigma)\langle l\,\frac{1}{2}\,m-\lambda,\lambda\,|\,jm\rangle. \quad (12)$$

Two identical nucleons in a j^2 configuration only

[11] D. M. Brink and G. R. Satchler, Nuovo Cimento 4, 547 (1956); A. de-Shalit and I. Talmi, *Nuclear Shell Theory* (Academic Press Inc., New York, 1963).

[12] In the notation of Ref. 7, if the radial form factor is chosen to be $F_{LSJ}(r)=I_L(r)$ then the spectroscopic coefficient is just

$$A_{LSJ}=-4\pi V_S 2^{1/2}(M_L\delta_{S0}+N_{LJ}\delta_{S1}).$$

Note also that the g_L defined in this reference is 4π times that used here.

have normal parity states, so that we must have $L=J$ for transitions of the type $(j^2)_{I=0}$ to $(j^2)_{I=J}$. However, since $j_1=j_2$ here, the first of Eqs. (11) shows that N_{LL} vanishes for this transition; there can be no spin flip. For $S=0$ transitions the standard reduction formulas[10,11] give

$$M_L=2(2L+1)^{-1/2}\langle lj\|T_{L0L}\|lj\rangle. \quad (13)$$

The ^{90}Zr ground state is a mixture

$$|0^+\rangle=a|p_{1/2}{}^2,0\rangle+b|g_{9/2}{}^2,0\rangle, \quad (14)$$

so the M_L for transitions to the excited states of the $g_{9/2}{}^2$ proton configuration are those given by Eq. (13) times the coefficient b. The numerical values are given in Table IV of the preceding paper.[1] The excited 0^+ state at 1.75 MeV is an exception because it is almost certainly a mixture complementary to the ground state (14), namely

$$|0^+,\ 1.75\ \text{MeV}\rangle=a|g_{9/2}{}^2,0\rangle-b|p_{1/2}{}^2,0\rangle.$$

For the excitation of this state we must have $L=J=0$, so that spin flip is forbidden here also. We soon find

$$\langle 0^+,1.75\|\textstyle\sum_i g_0T_{000}\|0^+,\text{GS}\rangle = (\pi)^{-1/2}ab[I_0(g_{9/2}{}^2)-I_0(p_{1/2}{}^2)]. \quad (15)$$

Other excited states may be formed by elevating one of the $p_{1/2}$ protons to the $g_{9/2}$ orbit. These transitions are of the form $(j^2)_{I=0}$ to $(jj')_{I=J}$, and for these we obtain

$$\langle (jj')J\|\textstyle\sum_i T_{LSJ}\|(j^2)0\rangle=[2(2j'+1)/(2J+1)(2j+1)]^{1/2} \times\langle l'j'\|T_{LSJ}\|lj\rangle. \quad (16)$$

Both components of the ground state (14) contribute to the excitation of the $(p_{1/2}g_{9/2})$ configuration. However, since[10]

$$\langle p_{1/2}\|T_{LSJ}\|g_{9/2}\rangle=(-)^{J-S}5^{1/2}\langle g_{9/2}\|T_{LSJ}\|p_{1/2}\rangle,$$

it is easy to see that the net result is to multiply the matrix element for the $(p_{1/2})^2$ to $(p_{1/2}g_{9/2})$ transition by the factor $[a+(-)^{J-S}5^{1/2}b]$.

Excitations of the hole-particle type[11] are formed by raising a nucleon from a filled shell into an unoccupied orbit. The final state can be represented as $|(j_h{}^{-1}j_p)J\rangle$, in an obvious notation. If only one type of nucleon is involved (such as in the excitation of a $g_{9/2}$ neutron in ^{90}Zr, leaving the protons in the $p_{1/2}$ orbit), the matrix element becomes[11]

$$\langle (j_h{}^{-1}j_p)J\|\textstyle\sum_i T_{LSJ}\|0\rangle=(-)^{J-j_h-j_p} \times[(2j_p+1)/(2J+1)]^{1/2}\langle j_p\|T_{LSJ}\|j_h\rangle. \quad (17)$$

If both neutrons and protons can participate (such as in the excitation in ^{90}Zr of a nucleon from the filled $p_{1/2}$ and lower shells), the hole-particle pair may be in a $T=0$ or $T=1$ state. The corresponding matrix elements are as in Eq. (17), times the factor $(-)^{T+1}[2/(2T+1)]^{1/2}$. Numerical values of the matrix elements M_L and N_{LJ} for a number of hole-particle excitations of interest in ^{90}Zr are given in Table IV of the preceding paper. Because of the ground-state mixture (14), the elements for excitations which leave the protons in the $p_{1/2}$ shell are multiplied by a, while those for final states in which two protons occupy the $g_{9/2}$ orbit are multiplied by b.

IV. NONLOCALITY

We have good reasons to believe that the optical-model and shell-model potential wells are nonlocal. It is known that scattering from a nonlocal well can be reproduced by an equivalent local potential, whose parameters will vary with the bombarding energy; at least part of the observed energy dependence of the empirical (local) optical potential is due to this nonlocality. The nonlocality, however, has another important effect on the wave function in the nuclear interior; the wave function for a nonlocal potential is reduced inside the nucleus compared to that for a local potential which gives the same scattering.[13] This reduction can be well represented by a damping factor obtained from the local energy approximation,[14]

$$G(r)=C[1-(\mu\beta^2/2\hbar^2)U(r)]^{-1/2}. \quad (18)$$

Here β is the nonlocality range, μ the reduced mass of the particle, and $U(r)$ is the equivalent local potential. The constant C is unity for scattering wave functions. The same reduction occurs for shell-model bound-state wave functions; if a radial function calculated in a local potential $U(r)$ is $u(r)$, then $\tilde{u}(r)$ for the same binding energy in the "equivalent" nonlocal potential is given by $\tilde{u}(r)=G(r)u(r)$. In this case, the constant C is obtained by demanding the new wave function remains normalized,

$$\int_0^\infty \tilde{u}(r)^2r^2dr=1.$$

Since $\tilde{u}(r)$ is reduced in the interior, we must have $C>1$ so that the tail of $\tilde{u}(r)$ is increased relative to that of $u(r)$. The energy dependence of the empirical optical potential for nucleons corresponds to $\beta\approx0.85$ F, and this value was used in all the present calculations. This gives an upper limit to nonlocality effects, insofar as some of the observed energy dependence may be intrinsic and not due to nonlocality.

V. THE RADIAL FORM FACTORS

Two finite-range forms were used for the radial dependence $g(r_{ip})$ of the effective interaction (1). The first is a Gaussian,

$$g(r)=\exp(-\gamma r^2). \quad (19)$$

[13] F. G. Perey, in *Proceedings of the Conference on Direct Interactions and Nuclear Reaction Mechanisms, Padua, 1962*, edited by E. Clementel and C. Villi (Gordon and Breach Science Publishers, Inc., New York, 1963); N. Austern, Phys. Rev. **137**, B752 (1965).

[14] F. G. Perey and D. Saxon, Phys. Letters **10**, 107 (1964).

This form has been used in a previous application of the shell model to proton scattering.[15] The second form is that of Yukawa,

$$g(r)=\exp(-\alpha r)/\alpha r. \tag{20}$$

These two are chosen because they yield analytic expressions for the multipole expansion (3) (see the Appendix). Calculations were also made for a zero-range potential with

$$V_S g(r)=A_S\delta(\mathbf{r}). \tag{21}$$

To compare interaction strengths for potentials of different ranges and different shapes it is convenient to use the volume integral of the potential,

$$A_S=V_S\int g(r)dr. \tag{22}$$

For zero range, the A_S are just the coefficients appearing in Eq. (21), while for the other forms we have

$$\begin{aligned} A_S&=V_S\times(\pi/\gamma)^{3/2}: \quad \text{Gauss}\\ &\times(4\pi/\alpha^3): \quad \text{Yukawa}. \end{aligned} \tag{23}$$

For orientation, we might note the parameter values for these interactions which fit low-energy nucleon-nucleon scattering data. These depend upon the angular-momentum states, but, for example, the $S=0$ part of the interaction (1) corresponds to 3/16 of the sum of the singlet and triplet even interactions if we assume a Serber exchange mixture. Then the values $\gamma\approx0.4$ F^{-2}, $V_0\approx24$ MeV, or $\alpha\approx0.8$ F^{-1}, $V_0\approx19$ MeV are indicated, and correspond to $A_0\approx500$ MeV F^{-3}. Further, a Serber mixture corresponds to strengths in the ratios

$$V_{0\alpha}:V_{0\beta}:V_{1\alpha}:V_{1\beta}=3:-1:-1:-1,$$

which gives, for example,

$$(V_{1\alpha}+V_{1\beta})=-(V_{0\alpha}+V_{0\beta}). \tag{24}$$

The single-particle radial wave functions $u_k(r)$ which appear in the expression (9) for the radial form factors $I_L(r)$ were computed[16] using a Saxon well of radius $r_0=1.20$ F, diffuseness $a=0.7$ F, and a spin-orbit coupling of 25 times the Thomas term (similar to the parameters of the real part of the optical potential[1] for ^{90}Zr+p). The Coulomb potential from a uniform charge of radius $1.25A^{1/3}$ F was included. The well depth was adjusted to give a binding energy of 5.68 MeV for the $1g_{9/2}$ proton, 6.60 MeV for the $2p_{1/2}$ proton; these required 61.9 and 59.2 MeV, respectively. The nonlocality correction of Eq. (18) was applied, assuming $\beta=0.85$ F. The constant C is 1.168 for the $1g_{9/2}$ and 1.165 for the $2p_{1/2}$; in the nuclear interior both functions are reduced by about 5% compared to the local potential values, but this corresponds to a damping of over 20% relative to the magnitude of the wave-function tail. Since $I_L(r)$ depends upon two of these radial functions, nonlocality leads to a substantial reduction in the importance of the contributions to $I_L(r)$ from the nuclear interior.

The $I_L(r)$ are sensitive to the range of the interaction. With the zero-range form (21), the g_L and hence the I_L

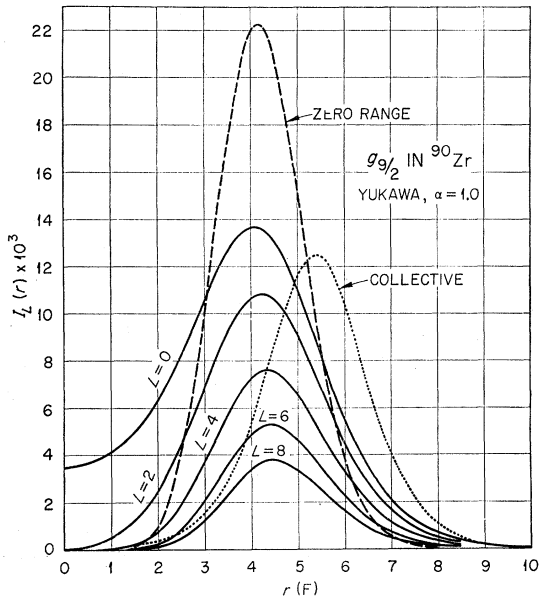

FIG. 1. Radial form factors for a $g_{9/2}$ proton in ^{90}Zr. The solid curves result from a Yukawa interaction of range 1 F. The dotted "collective" curve is proportional to the derivative of the real part of the optical potential (Ref. 1) and is arbitrarily normalized.

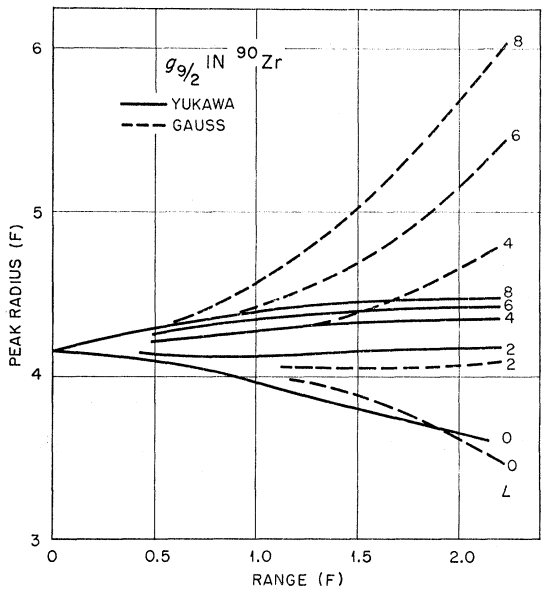

FIG. 2. Variation in position of the peaks of the various $I_L(r)$ with the range α^{-1} or $\gamma^{-1/2}$ of the interaction.

[15] H. O. Funsten, N. R. Roberson, and E. Rost, Phys. Rev. 134, B117 (1964).

[16] A code due to B. Buck was used for this.

are independent of L,

$$I_L(r)=u_2(r)u_1(r)/4\pi: \text{ zero range.} \quad (25)$$

As the range increases, the low-multipole form factors become larger than those for the high multipoles, while the high multipoles tend to peak at larger radii. An example is shown in Fig. 1 for transitions between $1g_{9/2}^2$ proton states (so that $u_1=u_2$), comparing results for a zero-range interaction with those for a Yukawa of range 1 F. The decrease in peak height with increasing L is very evident, but the variation in peak position with L is not very marked. This latter property is characteristic of the Yukawa shape, but the Gaussian is quite different in this respect. Figure 2 emphasizes this, again for a $1g_{9/2}$ proton. Except for the monopole, the Yukawa I_L peak positions vary little with range, while those for a Gaussian spread out considerably. Of course, the peaks become broader in both cases as the range increases.

Some examples of I_L for other transitions are shown in Fig. 3 for a Yukawa with $\alpha=1$ F. These indicate that a variety of shapes are possible, including changes in sign, which depend upon the single-particle wave functions involved. These I_L (and those for the other configurations discussed in the preceding paper[1]) were

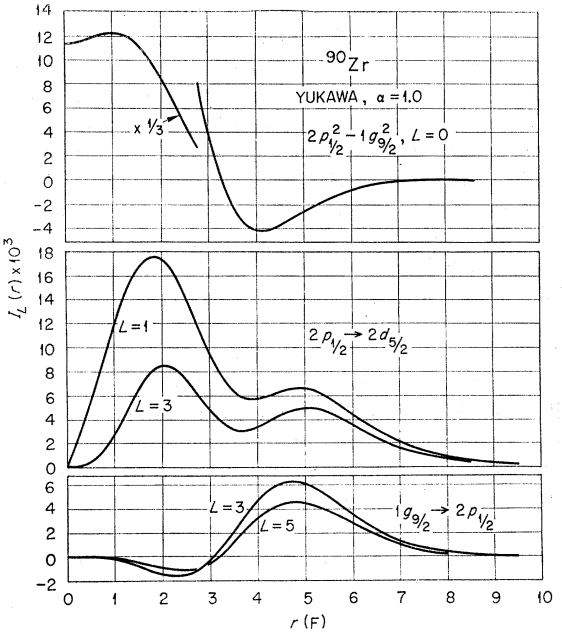

FIG. 3. Radial form factors for some other configurations in ^{90}Zr.

TABLE I. Well depths V and binding energies B for a proton bound in ^{90}Zr used in the calculations. Other potential parameters as described in the text.

Orbit	$1g_{9/2}$	$2p_{1/2}$	$2p_{1/2}$	$2p_{3/2}$	$1f_{5/2}$	$1f_{7/2}$	$3s_{1/2}$	$2d_{5/2}$
B (MeV)	5.68	6.60	7.75	9.65	9.46	14.30	2.15	0.35
V (MeV)	61.9	59.2	61.0	61.0	61.0	61.0	61.0	61.0

calculated assuming a proton moving in the same potential well as before, with the depth fixed at 61 MeV for orbits other than the $2p_{1/2}$ or $1g_{9/2}$; the corresponding binding energies are listed in Table I. Using this well depth for the $2p_{1/2}$ (which gives a binding energy of 7.7 MeV) instead of the 59.2 MeV required to give a binding of 6.6 MeV was found to have almost neligible effect.

It might be thought that the $I_L(r)$ for a neutron could differ appreciably from those for a proton between the same two orbits because of the large difference in binding energies. For example, in the $2p_{1/2}$ to $2d_{5/2}$ transition, the neutron single-particle states are bound by about 6 MeV more than those for the proton. If the binding energies are taken as 12.55 MeV ($2p_{1/2}$) and 7.20 MeV ($2d_{5/2}$), the well depths required are 50.4 and 53.8 MeV, respectively. Nonetheless, the corresponding $I_L(r)$ are almost identical. This results because the single-particle wave functions are themselves almost identical (except in the extreme tails). The deeper potential for the proton (due to the symmetry potential) and the Coulomb barrier just compensate the effects of the smaller binding energy. Of course, at large radii the two wave functions take on different asymptotic forms, but these are small in magnitude and contribute little to the I_L integrals.

Increasing the radius of the shell-model potential well to $1.25A^{1/3}$ F "expands" the wave functions slightly and has a similar effect on the resulting $I_L(r)$ form factors. Including the nonlocality correction (18) has much the same effect.

A more interesting comparison is between the use of harmonic oscillator wave functions and those for a Saxon well. The bulk of the more realistic function can be reproduced fairly accurately by an oscillator function with an appropriate choice of constant. For example, both the $1g_{9/2}$ and $2p_{1/2}$ functions used here agree quite closely with oscillator functions if $(\hbar/Mw)^{1/2}=2.1$ F, although, of course, the tails are different. The peak of the $1g$ oscillator function is a little broader than that for the Saxon well. The accuracy of the agreement is reduced as the number of nodes increases. The positions of nodes and antinodes can usually be made to agree, but the amplitude of the oscillations at small radii is relatively larger for the oscillator than it is for the flat-bottomed Saxon well. When these oscillator functions are used to construct the $I_L(r)$, we find rather small differences from those obtained with the Saxon-well eigenfunctions, even in the tails, when ranges $\gamma=0.293$ F^{-2} or $\alpha=1$ F^{-1} are employed. It appears that the finite range of the interaction determines the over-all shapes of the I_L and the wave-function tails have rather little effect. However, the peaks of the I_L for $1g^2$ are somewhat broader for the oscillator when the Gaussian interaction is used. The effect is small, but can have important consequences for the high-multipole cross sections (the $L=8$ cross section is increased by a factor of nearly 2

in the present case). Possibly a slightly smaller value of $(\hbar/M\omega)$ would improve the agreement with the Saxon-well results. The cross sections for the Yukawa interaction agree to within a few percent for all multipoles.

If we are studying transitions in nuclei close to closed shells where the single-particle energies are known, it would seem to be advisable to use the "realistic" wave functions. The results just quoted are reassuring in that we probably should not make *gross* errors if we used slightly incorrect wave functions, particularly with the Yukawa interaction. For example, the states of the $g_{9/2}^2$ configuration in ^{90}Zr cover an energy range of 3.6 MeV, but we use the same wave functions (corresponding to the separation energy from the ground state) for all the excited states. However, it is also clear that care must be taken if oscillator wave functions are used.

Finally it is of interest to compare the shell-model form factors discussed here with that given by the collective model. For first-order transitions the latter is just the derivative of the optical potential, and is complex. The real part is included in Fig. 1; it is symmetrical, peaks at 5.38 F and has a half-width of 2.4 F. The $I_L(r)$ for a $g_{9/2}$ proton, also shown in this figure, are considerably broader (I_2 has a half-width of 3.1 F), peak at about 1 F smaller radii, and have longer tails. Other transitions in which the orbit changes have I_L very different in shape from the collective interaction (see Fig. 3, for example).

VI. CROSS SECTIONS

In the distorted-wave approximation, the theoretical differential cross sections have the form[7]

$$d\sigma/d\omega=\sum_{LSJ} V_S^2\sigma_{LSJ}(\theta), \tag{26}$$

where

$$\sigma_{LSJ}(\theta)=(2J+1)(M_L^2\delta_{S0}+N_{LJ}^2\delta_{S1})\sigma_L(\theta). \tag{27}$$

Two approximations are implicit in these equations. When spin-orbit coupling is included in the distorted waves, there can be interference between different values of S and L when more than one is allowed. If spin-orbit coupling is omitted, these interferences vanish. Explicit calculations[17] show that they are also negligible when spin-orbit effects are included, so we omit them from Eq. (26). Further, we have found that the "single particle" cross section $\sigma_L(\theta)$ is independent of S and J to within a few per cent, so in Eq. (27) we assume it depends only on L. (We call σ_L a "single particle" cross section because it depends only on the radial parts of the two single-particle orbits involved in the transition. The remaining nuclear-structure information is contained in the matrix elements M_L or N_{LJ}.)

For the calculations reported here, the optical potential A of the preceding paper was used. Calculations with the "best-fit" potential showed very similar results except for an over-all reduction in cross section of about 10%. Nonlocal damping of the distorted waves was included in the approximation (18); this results in a reduction of the integrand of the transition amplitude by a factor 0.69 in the nuclear interior when $\beta=0.85$ is chosen. The effects on the cross sections are large. With a Yukawa of range $\alpha=1$ F^{-1}, the $g_{9/2}^2$, $L=2-8$ and $g_{9/2}p_{1/2}$, $L=5$ cross sections are reduced uniformly to about 2/3 their values when nonlocality is ignored, with essentially no change in angular distribution. However, the relative cross sections for different multipoles are strongly affected by the distorted-wave nonlocality corrections if a Gaussian with the roughly equivalent range of $\gamma=0.293$ F^{-2} is used. The $L=2$ cross section for the $g_{9/2}^2$ transitions is reduced by a factor 0.62 by nonlocality, while the $L=8$ cross section is reduced only by about 10%. This difference between Gauss and Yukawa can be traced to the difference in positions of the peaks of the corresponding $I_L(r)$ form factors (see Fig. 2). The I_L for the Yukawa all peak at approximately the same radius and hence tend to be affected in the same way, while the Gaussian I_L for large L peak at larger radii where the nonlocality correction is much smaller. Analogous differences in behavior could be expected under changes in optical-potential parameters; for example, an increase in the absorptive potential would dampen Yukawa cross sections for all L while the Gauss cross sections for low L would be most affected.

When fitting the experimental data for exciting the $g_{9/2}^2$ and $g_{9/2}p_{1/2}$ states,[1] the range of the interaction was varied until both the angular distributions and the relative cross sections for the various multipoles were reproduced satisfactorily. Figures 4 and 5 show the effects of range variation for the Yukawa form. To facilitate comparison, the "reduced" cross sections σ plotted are normalized using Eq. (23), so that

$$\frac{d\sigma}{d\omega}=A_S^2\sigma\times10^{-6}\times\begin{cases}b^2: & g_{9/2}^2\\ 1: & g_{9/2}p_{1/2}\end{cases}$$

gives the predicted cross section in (mb/sr) if A_S is in units of MeV F^{-3}. Of course, only $S=0$ is allowed for $g_{9/2}^2$. The $g_{9/2}p_{1/2}$ normalization assumes a ground-state mixture $a=0.8$, $b=-0.6$. The 5^- level may be excited both with ($S=1$) and without ($S=0$) spin flip. The normalization in Fig. 5 assumes only $S=0$. Provided the two parts of the interaction have the same range, the angular distribution is very insensitive to the presence of spin flip. It would seem that measurements of polarization, or p'-γ angular correlations, are required to identify spin flip unambiguously.

These figures illustrate two features. First, the strength of the high-multipole cross sections compared to the low multipoles is very sensitive to the range of the interaction. Secondly, the longer the range, the more structure appears in the angular distributions.

[17] R. M. Haybron (private communication).

These features are due to the greater radial spread of the $I_L(r)$ as the range increases. The lack of structure for zero rainge ($\alpha=\infty$), as well as the much too slow decrease in cross section with increasing L, rules out the zero-range interaction. For example, the ratio of $L=6$ to $L=2$ cross sections is about 7 times larger than observed experimentally. A reasonable compromise between agreement in shape and relative magnitudes is obtained with a range of about $\alpha=1$ F^{-1}. A comparison of experiment and theory with this range was shown in the preceding paper.[1] It required $|V_0|\simeq 205$ MeV, corresponding to $|A_0|\approx 2580$ MeV F^3. The fit to the 5^- angular-distribution shape was not good; indeed, no choice of α with a Yukawa reproduced this shape correctly. The addition of spin flip does not help, because the $S=0$ and $S=1$ angular distributions are almost identical and the interference between is negligible.[17]

The only interaction found in the present work to give a good fit to the 5^- angular distribution was a Gaussian with $\gamma=0.5$ F^{-2}. Unfortunately this gives a poor account of the other angular distributions, although the relative cross sections predicted are in fair agreement

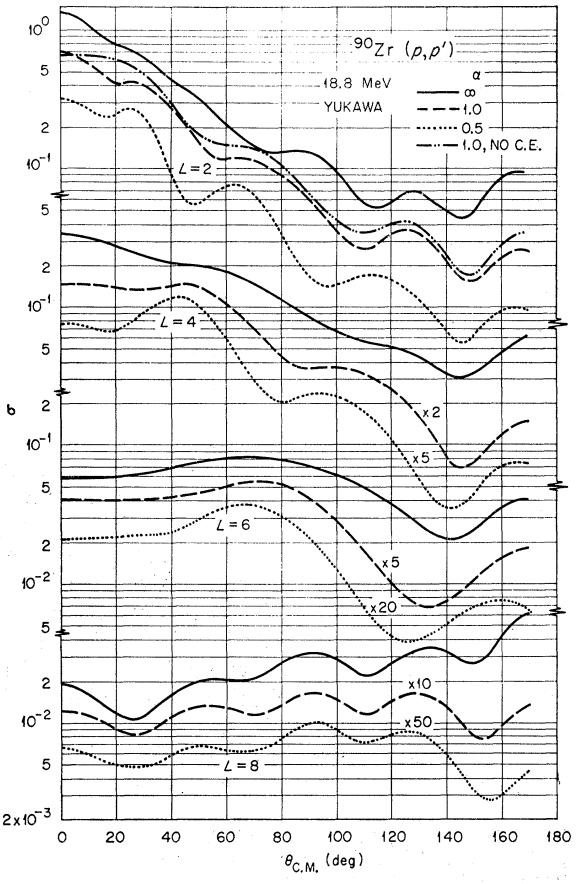

FIG. 4. Variation with range of the "reduced" differential cross sections predicted for excitation of the $g_{9/2}^2$ states with a Yukawa interaction. Coulomb excitation is included for the $L=2$ curves except where noted.

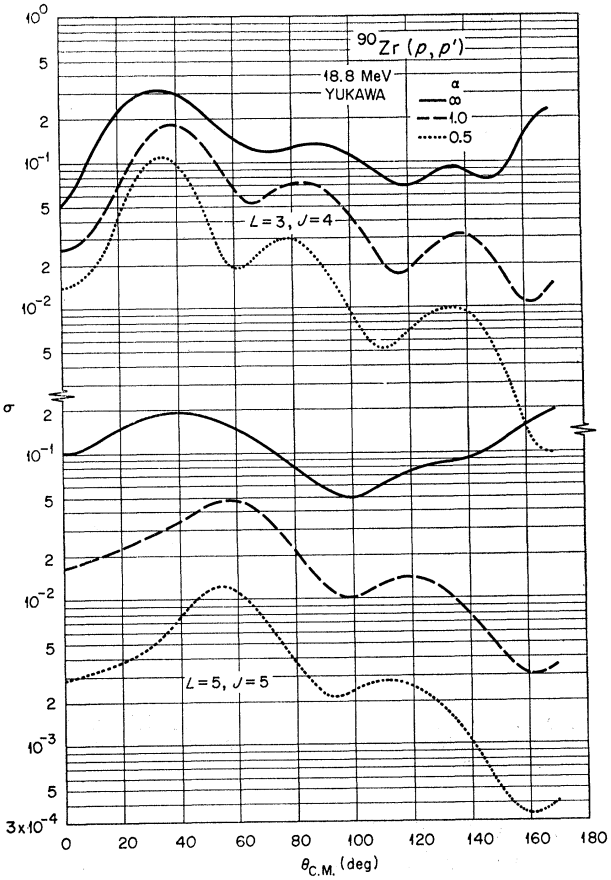

FIG. 5. Variation with range of the "reduced" differential cross sections predicted for excitation of the $g_{9/2}p_{1/2}$ states with a Yukawa interaction.

with experiment. Figure 6 compares some predicted cross sections for the $g_{9/2}^2$ and $g_{9/2}p_{1/2}$ states using the Yukawa with $\alpha=1$ F^{-1} and she Gaussian with $\gamma=0.293$ and 0.5 F^{-2}. The curves for various interaction shapes and ranges show a close qualitative similarity to each other, but the differences are enough for a reasonably accurate experiment to distinguish between them.

We have already discussed the effects on the cross section of the nonlocal damping of the distorted waves. The effects of the nonlocal corrections to the single-particle bound states are of particular interest because we have little direct evidence about the nonlocality of the shell-model potential. Evidence from $(p,2p)$ reactions on the energies of deeply bound orbits indicates the shell-model potential is energy dependent to about the same extent as the optical potential. Nonetheless we do not know how much of this is due to nonlocality. Further, the behavior of the least rightly bound orbits (with which we are concerned here) appears to be contrary to this energy dependence.[18]

[18] G. E. Brown, J. H. Gunn, and P. Gould, Nucl. Phys. **46**, 598 (1963); G. R. Satchler, unpublished. This work indicates that, if the other parameters of the well are kept fixed, the more strongly bound orbits require a more *shallow* well.

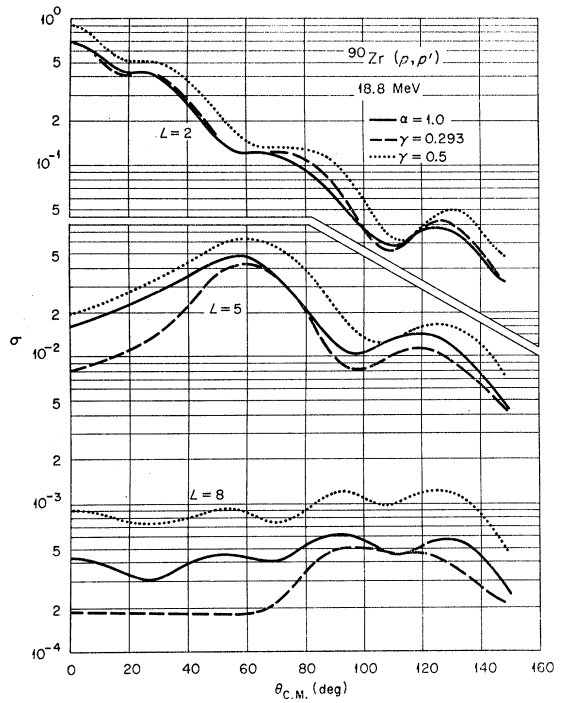

FIG. 6. Comparison of the "reduced" differential cross sections for Gaussian interactions of two different ranges with those for a Yukawa of range $\alpha^{-1}=1$ F.

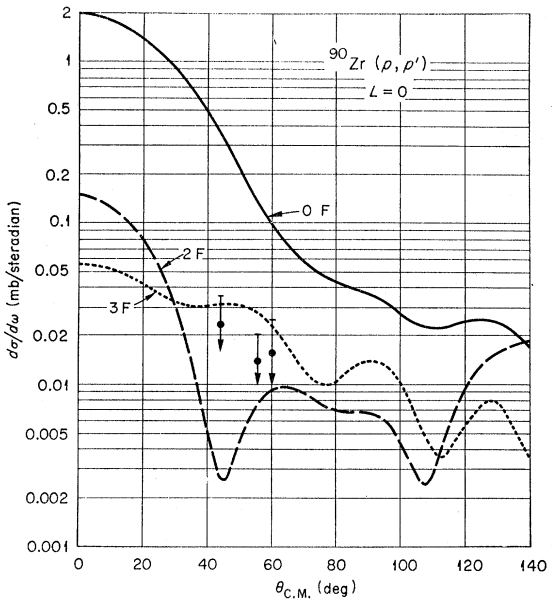

FIG. 7. Predicted cross sections for excitation of the 0^+ level at 1.75 MeV using a Yukawa interaction of range $\alpha^{-1}=1$ F. The numbers on the curves refer to cutoff radii. The experimental points are upper limits only (Ref. 1).

With a Gaussian interaction, $\gamma=0.293$ F^{-2}, the low multipoles are little affected by the nonlocal correction to the bound-state wave functions. The cross section for $L=2$ and $g_{9/2}^2$ differs at most by 1 or 2%, whereas the $L=8$ cross section is increased almost uniformly by about 25% by the nonlocal correction. The Yukawa predictions, however, are affected less, the cross section being changed by only a few percent for all multipoles. This behavior can be understood when we remember that nonlocality increases the magnitude of the single-particle wave-function tail (by 1.168 for the $g_{9/2}$ orbit) and hence also the $I_L(r)$ in the surface region which usually contributes most to the reaction. As Fig. 2 shows, the I_L for a Yukawa tend to peak at about the same radius, so all L are affected rather similarly, whereas the Gaussian I_L for large L peak at larger radii and are increased more by the nonlocality than those for small L.

A special case is provided by the 0^+ state at 1.75 MeV. As already described in Sec. III, its wave function is probably the complement of that for the ground state and the nuclear matrix element (15) for its excitation is proportional to the difference between the I_0 for $g_{9/2}^2$ and $p_{1/2}^2$. Figure 3 shows this radial form factor for a Yukawa with $\alpha=1$ F^{-1}, and Fig. 7 shows the predicted cross section for the strength $V_0=205$ MeV which fits the other $g_{9/2}^2$ states. The experimental data are only upper limits, but we see that the predictions are an order of magnitude larger. (Coulomb-excitation contributions are very small and do not affect this result.) This result seems fairly general, occurring for both Gauss and Yukawa for all the ranges studied, and is not altered by reasonable changes in the single-particle wave-function parameters. The largest contribution to the amplitude comes from the large peak in $I_0(g^2)$-$I_0(p^2)$ near $r=0$ (see Fig. 3). If the radial integrations in the distorted-wave amplitude are cut off so that contributions from $r<2$ F or $r<3$ F are eliminated, the cross sections are greatly reduced (Fig. 7). Multipoles with $L>0$ received little contribution from this central region; the cutoff at 3 F only slightly affects the $L=2$ cross section. However, the justification for such a cutoff is obscure. It is possible that the true effective interaction is much weaker within nuclear matter.[5] On the other hand the discrepancy may arise because the true monopole strength is inadequately represented by our simple interaction. It may be necessary, for example, to include a repulsive core in the interaction, although no serious attempts have been made to obtain fits to the data in this way because it introduces at least one new parameter.[19] More complete measurements on the 0^+ excitation could be helpful in resolving some of these questions.

Finally, let us compare the present shell model with the collective model. It was shown in the preceding

[19] See, for example, F. Coester and E. Yen, Nuovo Cimento **30**, 674 (1963). Calculations were made for the effective interaction suggested by these authors. It gives cross sections of the right order of magnitude (within a factor of 3 or so) but neither the angular distributions nor the *relative* cross sections for the $g_{9/2}^2$ states are reproduced. These discrepancies are due to the very short range of this interaction.

paper[1] that the real part of the collective-model interaction (whose radial shape is shown in Fig. 1) gave a good fit to the measured $L=2$ transition to the 2^+ state of the $g_{9/2}{}^2$ configuration. An equally good fit was obtained with the shell model using $\alpha=1.0$ F^{-1}, yet Fig. 1 shows these are obtained with very different radial form factors. This illustrates one of the difficulties of interpreting the data. It may be easy, within the constraints imposed by a given model, to determine the parameters which give a good fit to the data, but this does not rule out the possibility of a quite different model giving equally good fits. Indeed the collective model fits the other $g_{9/2}{}^2$ and $g_{9/2}p_{1/2}$ transitions as well as, if not better than, the shell model in the form used here. On the other hand, the deformation parameters so obtained are not related in any simple way and do not provide the consistency check on the various multipole strengths that the more detailed shell model gives.

One of the most interesting features of the collective model is that the interaction it gives is complex, and the experimental data (at least for the strong transitions which have received most analysis) demand that the imaginary part be included. It remains to be seen whether it will be necessary to introduce a complex effective interaction with the shell model, or whether this is only required for the so-called collective transitions. It is worth remembering that the impulse approximation gives a complex interaction operator.

ACKNOWLEDGMENTS

We are indebted to R. M. Drisko for the use of the distorted-wave code JULIE and to B. Buck for the subroutine to calculate bound-state wave functions. Many helpful discussions were held with R. H. Bassel and R. M. Drisko. M. L. McFadden and R. J. Metzger assisted with the calculations.

APPENDIX

The multipole expansion (3) has simple analytical forms for a number of cases. For very long range, $g(r_{ip})=$constant, only the monopole $g_0(r_i,r_p)$ survives and it has the same constant value. In the limit of zero range, $g(r_{ip})=\delta(\mathbf{r}_{ip})$, we have[10]

$$g_L(r_i,r_p)=\delta(r_i-r_p)/4\pi r_p{}^2$$

independent of L. The Gaussian,

$$g(r_{ip})=\exp(-\gamma r_{ip}{}^2),$$

yields the multipole terms

$$g_L(r_i,r_p)=\exp[-\gamma(r_i{}^2+r_p{}^2)](\pi/2ix)^{1/2}i^{-L}J_{L+1/2}(ix),$$

where $x=2\gamma r_i r_p$. These may be generated from the recurrence relation

$$g_{L+2}=g_L-(2L+3)x^{-1}g_{L+1}.$$

The expansion coefficients for the Yukawa form,

$$g(r_{ip})=(\alpha r_{ip})^{-1}\exp(-\alpha r_{ip}),$$

may also be expressed in terms of Bessel functions[20]

$$\begin{aligned} g_L(r_i,r_p)&=\alpha^{-1}(r_i r_p)^{-\frac{1}{2}}K_{L+1/2}(\alpha r_i)I_{L+1/2}(\alpha r_p), \quad \text{if } r_i\geq r_p,\\ &=\alpha^{-1}(r_i r_p)^{-\frac{1}{2}}K_{L+1/2}(\alpha r_p)I_{L+1/2}(\alpha r_i), \quad \text{if } r_i<r_p. \end{aligned}$$

These also satisfy recurrence relations,

$$\begin{aligned} K_{L+5/2}(x)&=K_{L+1/2}(x)+(2L+3)x^{-1}K_{L+3/2}(x),\\ I_{L+5/2}(x)&=I_{L+1/2}(x)-(2L+3)x^{-1}I_{L+3/2}(x). \end{aligned}$$

Numerical values of the Gaussian g_L and of the I were obtained by using a power series expansion for $x\leq 0.15$. Downward recursion was used for $0.15<x<10$, and upward recursion for $x\geq 10$. Upward recursion was used for the K for all x.

The Coulomb interaction $g(r_{ip})=r_{ip}{}^{-1}$ was needed for Coulomb excitation calculations. This has the well-known expansion

$$\begin{aligned} g_L(r_i,r_p)&=(2L+1)^{-1}r_p{}^L/r_i{}^{L+1}, \quad \text{if } r_i\geq r_p,\\ &=(2L+1)^{-1}r_i{}^L/r_p{}^{L+1}, \quad \text{if } r_p>r_i. \end{aligned}$$

Examination of the behavior with small values of the arguments of the g_L for finite-range interactions shows the corresponding $I_L(r_p)$ are proportional to $r_p{}^L$ for small r_p. The zero-range case is an exception; for this the $I_L(r_p)$ go like $r_p{}^{l_1+l_2}$ near the origin.

[20] G. Petiau, *La Théorie des Fonctions de Bessel* (Centre National de la Recherche Scientifique, Paris, 1955).